

GEOCHEMISTRY AND TECTONO-MAGMATIC SIGNIFICANCE OF HP/LT METAOPHIOLITES OF THE ATTIC-CYCLADIC ZONE IN THE LAVRION AREA (ATTICA, GREECE)

Adonis Photiades* and Emilio Saccani**[✉]

* *Institute of Geology and Mineral Exploration (IGME), Athens, Greece.*

** *Dipartimento di Scienze della Terra, Università di Ferrara, Italy.*

✉ *Corresponding author: e-mail: sac@unife.it*

Keywords: *geochemistry, MORB, calc-alkaline, Attic-Cycladic zone. Greece.*

ABSTRACT

The Lavrion area corresponds to the northwestern end of the Attic-Cycladic Complex and mainly consists of metamorphic rocks formed during the Eocene high-pressure/low-temperature (HP/LT) event and the Upper Oligocene-Lower Miocene medium-pressure metamorphic event. These metamorphic rocks are found in two superimposed tectonic units: the Kamariza Unit, which includes metavolcanic rocks and the overlying Lavrion blueschist Unit, which is largely represented by metaophiolites.

Protoliths of metavolcanic rocks in the Kamariza Unit are calc-alkaline basalts displaying a marked enrichment in Th, U, and LREE and depletion in Ta, Nb, Hf and Ti, which point to a genesis from a depleted mantle source further enriched by subduction components. The Lavrion blueschist Unit mainly includes metavolcanic rocks with tholeiitic composition, as well as subordinate metagranites and metavolcanic rocks with calc-alkaline affinity. The tholeiitic metavolcanic rocks are mainly represented by enriched-type (E-) mid-ocean ridge basalts (MORB) and subordinately by normal-type (N-) MORB. E-MORB chemistry implies a genesis from a depleted asthenospheric source modified by an OIB component, whereas the N-MORB has chemical features typical for rocks generated in a mid-ocean ridge setting from a primitive asthenospheric source.

Previous works suggested that the magmatic protoliths of similar HP/LT metamorphic rocks from elsewhere in the Cyclades reflect an arc-back-arc tectonic setting, which developed during the Cretaceous closure of the Pindos oceanic basin. However, recent geological studies have shown that the Lavrion metamorphic Units, unlike similar units from the Cycladic zone, represent Triassic Pelagonian sequences metamorphosed under HP/LT conditions typical of the Cycladic zone. The geochemical and petrological characteristics of the Lavrion metamorphic rocks support this conclusion. In particular, calc-alkaline protoliths display many similarities with the Triassic calc-alkaline rocks associated with the rift of Gondwana, whereas MORB-type protoliths are similar to the Triassic MORB found in the Subpelagonian ophiolitic mélanges. The magmatic protoliths of the Lavrion HP/LT metamorphic rocks are thus compatible with a paleotectonic evolution which encompasses the Triassic continental rift, followed by the early oceanization stage of the Pindos ocean, and emplaced on the border between the Pelagonian continental margin and the Pindos basin. These rocks were probably included into mélanges during the Jurassic closure of the Pindos basin, and finally they were involved in the Eocene and Upper Oligocene-Lower Miocene metamorphic events that affected the Cycladic zone.

INTRODUCTION

The Lavrion area (or Lavreotiki Peninsula) constitutes the northwestern part of the Attic-Cycladic Metamorphic Complex (Fig. 1), which largely consists of high-pressure/low-temperature (HP/LT) metamorphic rocks, including blueschists. Previous works carried out on these rocks in the Cycladic and Evia islands (e.g., Brocker, 1991; Seck et al., 1996; Katzir et al., 2000; Mocek, 2001) have suggested that the Attic-Cycladic Metamorphic Complex includes Mesozoic carbonates, clastic and magmatic protoliths, the latter being represented by island arc calc-alkaline sequences and magmatic rocks formed in a mid-ocean ridge setting (MORB). The metamorphic history of these rocks includes an Eocene HP/LT event and an Upper Oligocene-Lower Miocene medium-pressure metamorphic overprint (Katzir et al., 2000, and references therein). The occurrence of both calc-alkaline and MORB protoliths throughout the Cycladic zone has been interpreted by many authors as reflecting the pristine occurrence of an arc-backarc environment developed during the Middle-Upper Jurassic closure of the Pindos or Vardar Neo-Tethyan oceanic basin (e.g., Katzir et al., 2000; Mocek, 2001). In contrast with previous interpretations, recent geological data from the Lavrion area (Photiades and Carras, 2001) suggest that the protoliths of the HP/LT metamorphic rocks in this area were incorporated into sedimentary sequences during

two different tectonic events, prior to the Eocene HP/LT metamorphic event. According to these data, the magmatic protoliths of the metamorphic rocks from the Lavrion area would have recorded the magmatic events that occurred from the Triassic continental break-up (e.g., Pe-Piper, 1998) to the Triassic-Jurassic early stage of formation of the Pindos oceanic basin (e.g., Saccani and Photiades, 2005), rather than the final convergence phases that affected this Neo-Tethyan oceanic basin.

In this paper the nature of the magmatic protoliths of the metamorphic rocks from the Lavrion area are investigated in order to evaluate their tectono-magmatic significance in the framework of the geodynamic evolution of the Neo-Tethyan ocean in the Hellenide sector.

GEOLOGICAL SETTING

The Lavrion area is located in the SE part of Attica (Figs. 1, 2) and, together with the south Evia Island, represents the NW end of the Cycladic zone (Fig. 1). In this area, the Cycladic zone is characterized by widespread occurrence of HP/LT metamorphic rocks, the protoliths of which include carbonate, siliciclastic, volcanic rocks, and ophiolitic mélanges. This rock association probably represents a Mesozoic transition between a continental margin and an oceanic domain (Katzir et al., 2000).

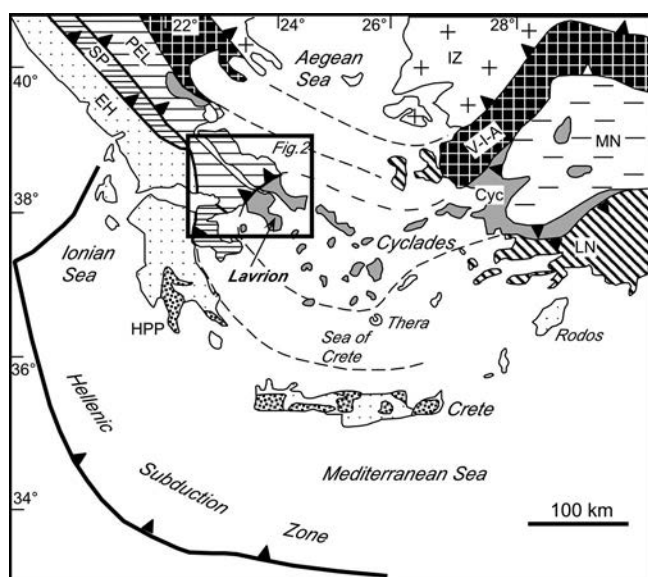


Fig. 1 - Simplified tectonic map of the Aegean area (modified from Ring et al., 2001). Abbreviations: EH- External Hellenides (Preapulian, Ionian, Gavrovo, Pindos zones); HPP- high pressure plattenkalk and phyllite-quartzite units; SP- Subpelagonian zone; PEL- Pelagonian zone; V-I-A- Vardar-Izmir-Ankara zone; IZ- Internal zones (Serbo-Macedonian, Rhodope); Cyc- Cycladic zone; MN- Menderes nappe; LN- Lycian nappe. The location of the Lavrion (Lavreotiki) peninsula and the area expanded in Fig. 2 are also reported.

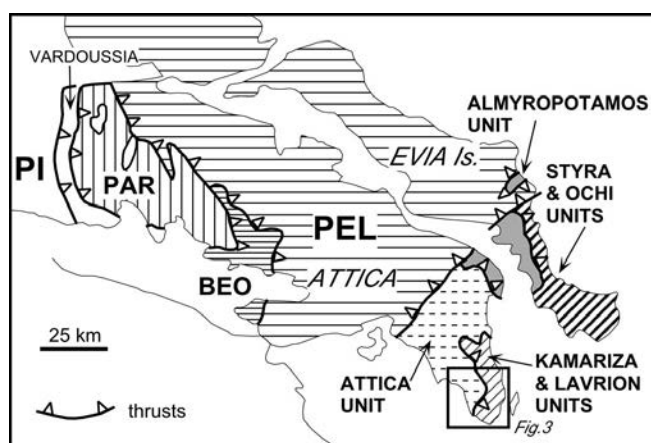


Fig. 2 - Tectonic map of the Attica and Evia areas (modified from Photiades and Carras, 2001). PI- Pindos zone; PAR- Parnassus zone; BEO- Beotian zone; PEL- Pelagonian zone.

Recent lithostratigraphic studies (Photiades and Carras, 2001) and the revised geological mapping at the scale 1:50.000 of the Lavrion sheet (Photiades et al., 2004) indicate that the Lavrion area (Fig. 3) consists of three superposed tectonic units, which were emplaced during the alpine phase. These tectonic units are, from bottom to top (Fig. 4):

- a lower para-autochthonous unit: the Kamariza Unit;
- a middle blueschist unit: the Lavrion blueschist Unit;
- an upper unit consisting of non-metamorphic outliers correlated to the Pelagonian domain.

The Kamariza Unit (Figs. 3 and 4) consists of Kamariza Marbles, representing a Triassic-(?)Lower Jurassic carbonate platform, covered by the Kamariza Schists, which represent a Jurassic volcano - sedimentary deposit.

According to Photiades and Carras, (2001), Photiades (2003) and Photiades et al. (2004), the metamorphic se-

quence forms a recumbent synclinal fold, where the limits are represented by the lower and upper Kamariza Marbles, respectively; and the core is occupied by the Kamariza Schists. The upper and lower marble sequences display identical fossil content and age (Marinos, 1955; Katsikatsos, 1977).

The Kamariza Schists have the following mineral assemblage: quartz, albite, white mica, and chlorite, and display granoblastic to lepidoblastic textures. Photiades and Carras (2001) suggested that these schists represent a volcano-sedimentary mélangé formed in a Jurassic basin characterized by clastic sedimentation, which developed in consequence of the collapse of the platform related to the closing of the Pindos or Vardar oceanic basin. The Kamariza Schists also include redeposited fragments of the carbonate platform, as well as (toward the top) ophiolitic volcanic bodies (Marinos and Petrascheck, 1956; Leleu, 1966; 1969). On the basis of the occurrence of mafic and ultramafic ophiolitic bodies Sindowski, (1948) suggested that this formation originated from the Internal Hellenides.

The Kamariza Unit has been metamorphosed under greenschist to amphibolite facies conditions and folded by an Upper Jurassic dynamometamorphic phase (Marinos and Petrascheck, 1956; Paraskevopoulos, 1957; Leleu, 1966) corresponding to the Eohellenic orogenic event, which has affected the Internal Hellenides (Vergely, 1984).

The metamorphic sequence is transgressively topped by an unmetamorphosed calcareous formation (up to 50 m thick), which lies either on the "Upper" Marbles, or directly on the Kamariza Schists (Fig. 4). It consists of conglomerates followed by limestones. When the calcareous formation overlies the marbles, the substratum frequently presents some dissolution cavities filled with conglomerates. The conglomerate contains reworked schist and marble pebbles from the underlying rocks. Limestones range from massive to thick-bedded and are slightly recrystallized and dolomitized. According to Photiades and Carras, (2001), this transgressive calcareous formation has a Late Jurassic - Early Cretaceous age.

The position of the Kamariza Unit within the Hellenides is still subject of debate. According to some authors (Leleu and Neumann, 1969; Katsikatsos, 1977; Marinos et al., 1977), this unit and the Evia Almyropotamos Unit (Fig. 2) have been indirectly considered to belong to the Internal Hellenides. Other authors (e.g., Katsikatsos et al., 1986) ascribe the Kamariza and the Almyropotamos Units to the External Hellenides, whereas Papanikolaou (1984) ascribes the Almyropotamos Unit to the External Hellenides and the Kamariza para-autochthonous to the Internal Hellenides. Photiades and Carras, (2001) concluded that the Kamariza Unit represents a para-autochthonous unit, which has all the features of the Internal Hellenides and is not related to the lithological series of Olympos - Ossa - Almyropotamos, pertaining to the External Hellenides and surfacing as tectonic windows within the Internal Hellenides. These authors also suggested that the Kamariza Unit, similarly to the Pelagonian domain, was affected by an Upper Jurassic orogenic episode.

The Lavrion blueschists Unit. This unit (also known as "Phyllite Nappe", Marinos and Petrascheck, 1956) is 100 to 250 m thick and is in tectonic contact above the para-autochthonous Kamariza Unit. In particular, it overlies the transgressive calcareous formation of the Kamariza Unit in the eastern part, and lies directly on the lower marble series to the west (Fig. 4). This unit consists of different metamor-

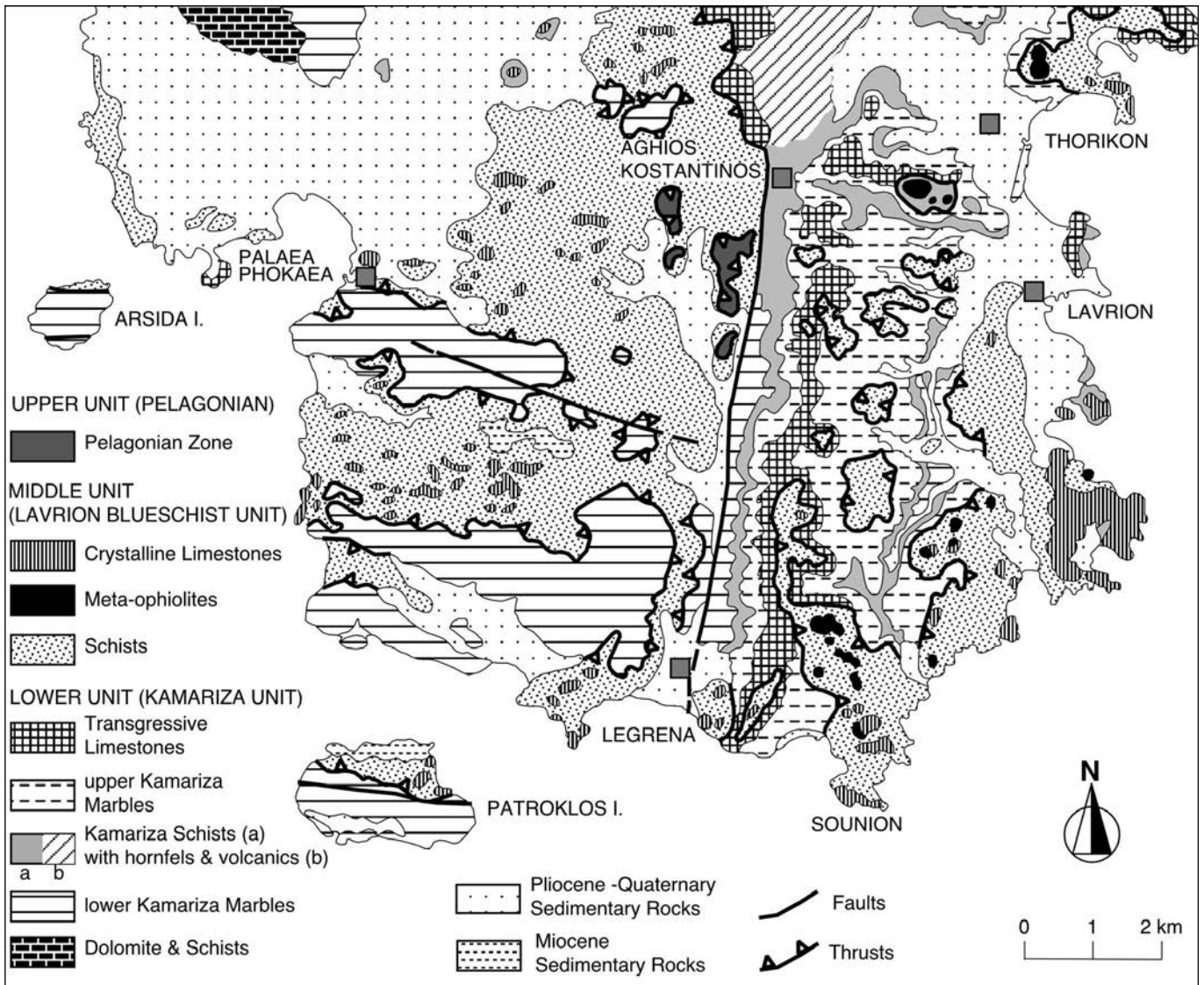


Fig. 3 - Simplified geological map of the Lavrion area (Lavrion Peninsula). Modified after Photiades and Carras (2001).

phic rocks, which are (from bottom to top): schists, metaophiolitic mafic rocks, and marbles (Fig. 4). Schists are intensely crenulated and have the following mineral assemblage: quartz, albite, white mica, glaucophane, epidote, and chlorite. Quartzites are also usually found as lenses quite often passing to quartziferous schists. Metaophiolites are represented by metabasalts and metagabbros rich in glaucophane (also reported as prasinite, metadiabase and metagabbro, Baltatzis, 1996; Arikas et al., 2001). These metaophiolites are often schistose and crop out mainly in the form of hillocks up to 10 m thick.

The blueschist unit comprises a Jurassic-Cretaceous succession, comparable with the Internal Hellenides and is characterized by Eocene blueschist facies metamorphism (Marakis, 1968; Altherr et al., 1982; Baltatzis, 1996). The blueschist facies is typical of the Attic-Cycladic metamorphic complex and originated under HP/LT conditions during the Alpine collision (Altherr et al., 1979; 1982; Maluski et al., 1980). The blueschist unit was emplaced on the Kamariza Unit during Middle-Late Miocene (Dermitzakis and Papanikolaou, 1980; Alexopoulos et al., 1998) and underwent a Miocene retrograde greenschist facies event related to a granodioritic (Plaka granodiorite) intrusion (Marakis, 1968; Baltatzis, 1981; Altherr et al. 1982).

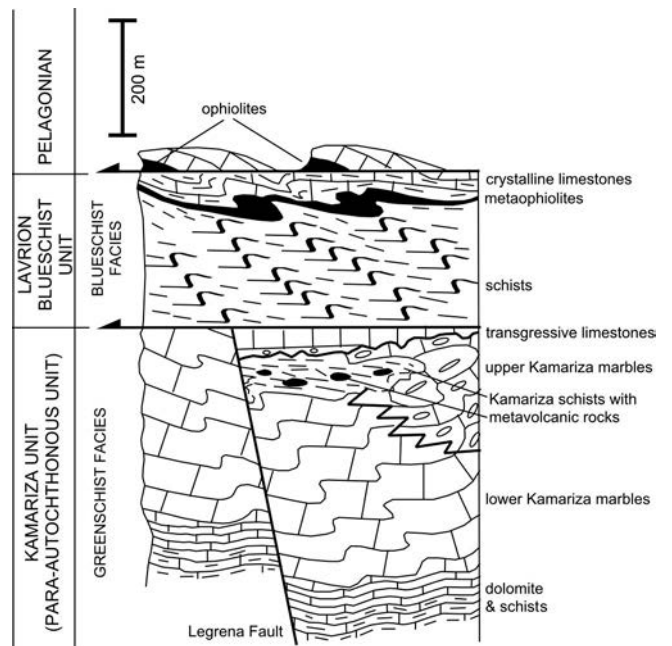


Fig. 4 - Simplified tectono-stratigraphic scheme of the Lavrion area (Lavrion Peninsula). Modified after Photiades and Carras (2001).

The upper unit representing Unmetamorphosed Pelagonian Sequence. This unit crops out as klippen up to 50 m thick and was emplaced on the previously described units during the Late Miocene. It is formed by thrust slices bearing ophiolitic relics (radiolarian cherts and serpentinites) at the base, and Cretaceous limestones at the top (Photiades and Carras, 2001). This unit is identical to some unmetamorphosed Mesozoic units representing part of the Pelagonian domain (Internal Hellenides) in continental Greece as, for example, the Lechonia Unit in Pelion (Ferrière, 1982), the Rhodiani area in the Vourinos Massif (Photiades and Pomoni-Papaioannou, 2001), the Argolis area (Bortolotti et al., 2003) and the Ano Vermio Unit in the Vermion Massif (Photiades, 2004). The upper unit of the Lavrion area is also comparable with the unmetamorphosed upper units found above the Attic-Cycladic metamorphic complex (Dürr et al., 1978; Papanikolaou, 1984).

SAMPLING AND METHODS

35 samples were collected from the metavolcanic rocks associated to the Kamariza Unit, and 27 samples were taken from the Lavrion blueschist Unit, including metavolcanic rocks and metagranites metamorphosed in both blueschist and greenschist facies from various localities.

Samples were analyzed for major and trace elements by X-ray fluorescence (XRF) on pressed-powder pellets, using an ARL Advant-XP automated X-ray spectrometer with the matrix correction method proposed by Lachance and Trail (1966). Accuracy and detection limits were determined using results from International Standards. Accuracy is generally lower than 2% for major oxides and less than 5% for trace elements, the detection limits for trace elements range from 1 to 2 ppm. Volatiles were determined as loss on ignition (L.O.I.) at 1000°C. CO₂ was determined by simple volumetric technique (Jackson, 1958) on samples bearing secondary calcite. Accuracy for this technique was checked by analyzing 20 reference samples with different CO₂ contents; the mean relative percentage error obtained was 2.4%. Rare earth elements (REE), Sc, Nb, Ta, Th, Hf, and U contents were determined on 37 selected samples by inductively coupled plasma-mass spectrometry (ICP-MS) using a VG Elemental Plasma Quad PQ2 Plus. Accuracy and detection limits were calculated by analyzing a number of international standards as unknown. Accuracy varies from 1% to 8%, while detection limits are (in ppm): Sc = 0.29; Nb, Hf, Ta = 0.02; REE < 0.14; Th, U = 0.01. All analyses were performed at the Department of Earth Sciences of the University of Ferrara. Results are presented in Tables 1 and 2.

PETROGRAPHY

The Kamariza metavolcanic rocks have foliated, porphyroblastic, poikiloblastic, and spotted textures. The main mineralogical assemblage includes albite + epidote + chlorite + quartz ± actinolite ± opaque minerals ± calcite. Foliated varieties commonly display a crenulation cleavage marked by the alignment of chlorite ± actinolite minerals and compositional segregation of quartz and albite. In some foliated rocks, small areas with granoblastic texture can be observed. Porphyroblastic rocks are the predominant textural type. Porphyroblasts are commonly repre-

sented by epidote and albite; in some cases albite replaces pre-tectonic relics of magmatic plagioclase. The matrix of porphyroblastic rocks ranges from foliated with crenulation cleavage to granoblastic. The poikiloblastic type shows chlorite, epidote, and albite poikiloblasts and porphyroblasts within a foliated to granoblastic matrix. The spotted varieties are characterized by spots of chlorite and epidote ± actinolite.

In the Lavrion blueschist Unit, three petrological types have been identified.

a) Blueschists that display porphyroblastic, lepidoblastic, and granoblastic textures. The typical mineral assemblage is sodic amphibole + epidote + albite + chlorite + quartz ± actinolite ± opaque minerals. In the lepidoblastic varieties, the schistosity is defined by the alignment of sodic amphibole and chlorite, whereas the mineralogical banding involves an alternation of sodic amphibole and chlorite with quartz and albite. In the porphyroblastic varieties, porphyroblasts are represented by idioblastic sodic amphibole and epidote usually set in a fine-grained, foliated matrix consisting of chlorite, albite, and quartz. In these rocks, sodic amphibole locally displays acicular texture. The granoblastic varieties are observed in some MORB-type rocks (see next chapter) and are characterized by extremely fine-grained textures. All analyzed samples display retrograde metamorphism testified by the growth of chlorite ± actinolite.

b) Chlorite-schists that display mainly granoblastic and subordinate porphyroblastic textures. The typical mineral assemblage in the porphyroblastic textural types is albite + epidote + chlorite + quartz ± actinolite ± opaque minerals. The modal proportions are variable, but chlorite is always the most abundant phase. Accessory phases are represented by titanite, apatite and rutile. Granoblastic varieties are commonly characterized by extremely fine-grained textures. Porphyroblasts in the porphyroblastic rocks are represented by epidote and magmatic plagioclase relicts set in a fine-grained granoblastic matrix. One sample (GE3) exhibits granulitic relics with clinopyroxenes of granoblastic polygonal texture.

c) Metagranites show well preserved granitic textures. The mineral assemblage is quartz + albite + sodic amphibole + chlorite + opaque minerals. Chlorite is very fine-grained and disseminated throughout the rock, whereas sodic amphibole displays decussate texture.

GEOCHEMISTRY

Many samples display secondary calcite veins; major-element composition has therefore been normalized to 100 wt% on a volatile- and secondary calcite-free basis for a better comparison of chemical data; these are the analyses we will be using from here on. In detail, CaO in calcite has been calculated according to stoichiometric proportions with CO₂ contents. The major element composition has then been re-calculated to 100 wt% without considering L.O.I. and CaO in calcite.

The chemical composition of the original magmatic rocks has most likely been changed by secondary alteration processes (e.g., seawater alteration) and/or during metamorphic transformations. For this reason, the following discussion is mainly based on relatively immobile elements, such as, Ti, P, Nb, Zr, Y, Hf, Th, Ta, and rare earth elements (REE), as well as transition metals (Ni, Co, Cr, V).

Table 1 - Bulk rock major and trace element analyses of representative metavolcanic rocks from the Kamariza Unit.

Sample Rock Note	SP2B bas	SP3B bas	SP6C bas and	SP7C bas	SP8C bas cc	SP8D bas and cc	SP8G bas cc	SP8K bas cc	SP10 bas cc	SP11 and cc	SP15 bas	SP15C bas cc	SP15D bas cc	SP16C bas cc	SP18A bas and cc	SP18L bas
<i>XRF Analyses:</i>																
SiO ₂	44.74	39.71	47.55	46.04	40.67	47.57	30.13	39.90	45.00	35.28	41.25	28.34	23.40	33.38	47.33	39.97
TiO ₂	1.51	1.47	1.53	1.12	1.46	1.57	1.18	1.33	1.58	0.85	1.73	0.65	0.61	1.04	1.54	1.47
Al ₂ O ₃	18.46	13.99	15.86	17.48	14.85	15.85	10.31	12.30	15.45	8.83	14.57	11.21	8.42	14.33	14.48	16.5
Fe ₂ O ₃	1.82	1.46	1.34	1.61	1.79	1.66	1.21	1.46	1.76	0.79	1.49	0.98	0.93	0.84	1.66	1.72
FeO	12.16	9.74	8.94	10.76	11.90	11.07	8.09	9.71	11.72	5.28	9.91	6.51	6.20	5.63	11.04	11.49
MnO	0.17	0.19	0.13	0.15	0.19	0.08	0.29	0.28	0.15	0.27	0.22	0.26	0.15	0.17	0.20	0.2
MgO	5.48	5.89	5.29	2.83	5.01	3.89	6.64	6.31	4.16	4.05	4.47	8.30	4.83	4.10	3.83	6.11
CaO	6.95	15.61	8.43	9.99	11.14	7.82	22.54	14.86	9.09	22.56	15.36	22.15	30.56	21.27	10.14	9.77
Na ₂ O	2.68	2.47	0.95	3.32	1.55	2.78	1.26	1.47	2.52	1.25	2.89	1.66	1.39	1.51	2.12	0.99
K ₂ O	0.69	0.55	1.63	0.68	1.31	1.67	0.42	0.76	1.07	0.50	0.50	0.90	0.26	1.54	0.72	3.15
P ₂ O ₅	0.30	0.29	0.36	0.16	0.09	0.42	0.17	0.15	0.08	0.19	0.26	0.10	0.08	0.33	0.41	0.04
L.O.I.	4.97	8.55	7.97	5.82	10.03	5.55	17.69	11.44	7.47	20.06	7.28	18.9	23.16	15.77	6.45	8.55
Total	99.95	99.91	99.97	99.96	99.99	99.94	99.94	99.97	100.03	99.91	99.93	99.96	100	99.91	99.92	99.97
CO ₂	1.94	6.35	4.55	3.01	7.12	3.37	13.86	8.60	4.60	13.71	4.99	16.78	20.50	13.33	3.27	5.16
Mg#	44.5	51.9	51.4	31.9	42.9	38.5	59.4	53.7	38.8	57.7	44.6	69.4	58.1	56.5	38.2	48.7
Zn	177	103	103	52	80	68	62	66	81	347	93	41	29	182	153	105
Cu	22	73	3	11	6	n.d.	6	66	27	2	51	n.d.	7	n.d.	13	1
Ga	16	14	19	10	11	11	10	10	14	12	15	3	2	20	17	14
Ni	n.d.	n.d.	n.d.	n.d.	n.d.	n.d.	n.d.	n.d.	3	n.d.	n.d.	2	2	n.d.	n.d.	6
Co	26	28	23	11	19	33	36	32	28	n.d.	22	22	22	n.d.	24	36
Cr	22	12	3	18	13	10	4	10	24	n.d.	14	22	20	2	5	21
V	359	344	216	296	117	182	150	155	175	56	344	67	284	58	212	142
Rb	22	12	58	14	29	35	10	20	28	11	10	19	4	33	20	65
Ba	143	133	118	87	96	93	41	70	77	91	127	50	24	178	190	146
Pb	16	5	22	2	n.d.	n.d.	n.d.	n.d.	n.d.	41	11	n.d.	2	5	6	2
Sr	281	230	53	175	65	66	85	65	61	149	302	127	282	192	242	89
Zr	161	128	188	88	105	121	76	100	113	117	163	22	25	201	210	103
Y	31	31	32	22	22	27	19	25	20	24	42	9	11	29	38	22
<i>ICP-MS Analyses:</i>																
Sc	29.7	30.5	27.2	26.7	32.3	36.2	32.2	34.3	27.6	16.1	36.0	24.6	23.9	20.3	32.1	31.7
La	20.2	24.0	36.1	12.2	11.4	18.6	17.1	13.7	11.5	25.2	22.2	5.2	7.00	28.4	34.5	11.8
Ce	45.6	51.6	71.8	26.9	25.6	36.4	32.3	32.8	25.5	44.4	49.9	11.7	14.4	53.6	69.8	27.2
Pr	5.73	6.37	9.18	3.45	3.61	5.48	4.67	4.38	3.05	6.37	6.41	1.53	2.01	7.31	9.59	3.50
Nd	25.5	28.3	35.9	16.0	16.3	23.4	19.1	18.9	13.7	25.4	27.9	6.07	8.55	29.5	35.5	17.0
Sm	5.38	7.57	10.1	3.54	4.07	7.37	6.02	4.59	3.30	6.16	6.22	1.63	2.16	6.91	9.74	3.70
Eu	1.52	2.22	2.45	1.08	1.16	2.30	1.87	1.44	1.04	1.61	1.76	0.50	0.65	1.55	2.46	1.20
Gd	5.64	7.46	9.45	3.64	4.12	7.25	5.84	4.79	3.36	6.29	6.19	1.62	2.15	6.79	9.10	3.84
Tb	0.96	1.32	1.61	0.63	0.72	1.37	1.08	0.80	0.58	1.02	1.07	0.29	0.36	1.07	1.50	0.69
Dy	5.23	7.99	9.42	3.60	4.09	7.97	6.24	4.92	3.38	5.64	6.27	1.65	2.12	5.79	7.86	3.91
Ho	1.07	1.53	1.71	0.72	0.84	1.46	1.16	1.01	0.65	1.20	1.34	0.36	0.45	1.21	1.55	0.80
Er	2.99	4.54	4.97	1.98	2.25	4.15	3.40	2.80	1.75	3.33	3.85	1.01	1.24	3.34	4.07	2.06
Tm	0.41	0.67	0.71	0.27	0.30	0.57	0.46	0.37	0.22	0.49	0.52	0.16	0.20	0.47	0.60	0.27
Yb	2.44	3.68	3.57	1.61	1.70	2.79	2.37	2.39	1.44	2.81	3.41	0.91	1.09	2.73	3.09	1.66
Lu	0.29	0.49	0.48	0.21	0.22	0.38	0.34	0.30	0.16	0.36	0.42	0.12	0.15	0.36	0.40	0.20
Nb	3.39	2.09	3.14	2.30	2.04	1.54	1.37	2.47	2.15	3.74	3.87	0.90	0.77	4.53	5.23	2.40
Hf	0.90	1.10	1.12	0.76	0.52	0.85	0.74	0.60	0.48	0.60	1.10	0.50	0.48	0.68	0.78	0.60
Ta	0.22	0.15	0.38	0.15	0.15	0.13	0.14	0.19	0.14	0.21	0.23	0.15	0.09	0.30	0.26	0.18
Th	5.19	4.90	6.45	2.65	1.97	2.48	1.96	2.50	2.22	3.75	5.82	1.06	0.99	7.16	5.80	2.20
U	0.94	0.47	0.75	0.42	0.19	0.87	0.51	0.97	0.88	0.88	0.63	0.10	0.21	0.89	0.73	0.21
Th/Ta	23.37	32.4	16.96	17.97	13.18	19.62	14.02	13.17	16.04	18.09	25.78	7.13	11.65	23.91	22.43	12.50
Th/Tb	5.41	3.72	4.00	4.24	2.73	1.81	1.82	3.12	3.81	3.68	5.43	3.71	2.73	6.68	3.87	3.18
Ba/Th	27.5	27.2	18.3	32.7	48.9	37.5	21.0	27.9	34.6	24.4	21.9	47.2	24.4	24.9	32.7	66.3
Th/Nb	1.5	2.4	2.1	1.2	1.0	1.6	1.4	1.0	1.0	1.0	1.5	1.2	1.3	1.6	1.1	0.90
Zr/Nb	47.4	61.5	59.8	38.2	51.3	78.3	55.7	40.3	52.6	31.3	42.1	24.6	32.1	44.3	40.1	43.0
Nb/Yb	1.39	0.57	0.88	1.43	1.20	0.55	0.58	1.03	1.49	1.33	1.13	0.99	0.70	1.66	1.69	1.45
(La/Sm) _N	2.42	2.05	2.32	2.23	1.82	1.63	1.83	1.93	2.25	2.64	2.31	2.08	2.08	2.65	2.28	2.05
(La/Yb) _N	5.94	4.67	7.26	5.46	4.84	4.80	5.19	4.13	5.73	6.44	4.67	4.13	4.59	7.47	7.99	5.08

Fe₂O₃ = FeO x 0.15; Mg# = 100 x Mg/(Mg + Fe²⁺), where Mg = MgO/40.32 and Fe = FeO/71.85. Normalizing values for REE ratios are from Sun and McDonough (1989). Abbreviations: bas- metabasalt; bas and- metabasaltic andesite; and- metaandesite; cc- occurrence of secondary calcite; n.d.- not detected.

Table 2 - Bulk rock major and trace element analyses of representative metamorphic rocks from the Lavri-on blueschists Unit.

Sample	Calc-alkaline Series				MORB Series				
	PI14	PI15	PI16	PI13	AF6	PL1	GE1	U4	GE6
Rock Type	bas gsct	and bsct	dac bsct	gra bsct	bas bsct	and bsct	Fe-bas bsct	Fe-bas bsct	bas gsct
Note					N-MORB	N-MORB	E-MORB	E-MORB	E-MORB
<i>XRF Analyses:</i>									
SiO ₂	51.74	57.16	60.94	63.58	43.12	58.87	44.14	47.64	49.05
TiO ₂	0.91	0.60	0.65	0.77	1.18	0.99	3.28	2.26	1.26
Al ₂ O ₃	19.83	21.05	19.56	17.44	15.45	15.39	11.67	14.26	13.02
Fe ₂ O ₃	0.91	1.01	0.66	0.66	1.28	1.38	2.21	1.90	1.36
FeO	6.07	6.71	4.39	4.37	8.53	9.23	14.71	12.70	9.04
MnO	0.12	0.05	0.03	0.08	0.23	0.06	0.66	0.13	0.18
MgO	6.59	1.74	1.02	1.06	15.01	2.46	7.42	9.58	9.98
CaO	3.57	0.46	0.92	1.03	6.19	1.90	5.77	4.22	10.39
Na ₂ O	2.77	6.56	8.33	8.63	2.15	5.14	3.52	3.30	3.02
K ₂ O	3.39	3.28	2.01	1.60	0.73	2.55	0.03	0.64	0.30
P ₂ O ₅	0.27	0.12	0.17	0.31	0.11	0.60	0.53	0.29	0.12
L.O.I.	3.79	1.34	1.42	0.60	5.92	1.50	5.78	3.02	2.35
Total	99.95	100.07	100.1	100.13	99.92	100.07	99.7	99.93	100.06
CO ₂	n.d.	n.d.	n.d.	n.d.	n.d.	n.d.	1.23	n.d.	n.d.
Mg#	65.9	31.6	29.3	30.2	75.8	32.3	47.3	57.3	66.3
Zn	98	87	56	92	98	99	149	126	85
Cu	10	23	6	4	52	43	41	40	98
Ga	13	12	13	14	17	2	25	10	4
Ni	12	8	4	14	122	69	37	25	95
Co	9	5	6	3	43	24	35	35	42
Cr	7	2	n.d.	n.d.	334	230	35	22	183
V	88	139	41	139	254	105	429	508	287
Rb	74	73	43	25	2	6	4	16	8
Ba	273	469	351	234	11	52	77	133	55
Pb	10	4	10	60	3	2	3	32	n.d.
Sr	117	23	59	9	138	35	48	134	129
Zr	157	269	261	320	51	106	257	171	60
Y	42	89	54	54	21	21	68	48	22
<i>ICP-MS Analyses:</i>									
Sc	22.9	26.4	22.8	13.1	35.0	53.0	32.3	43.8	37.8
La	31.0	18.6	12.0	24.7	2.18	2.81	15.9	11.5	8.36
Ce	65.6	47.3	27.8	52.7	7.64	10.2	40.5	26.9	17.1
Pr	8.41	7.08	4.26	7.10	1.59	1.76	5.56	4.42	2.49
Nd	40.1	30.6	18.3	32.7	8.19	9.41	27.0	21.2	11.1
Sm	10.4	7.54	4.70	8.55	2.45	2.78	7.56	5.87	2.88
Eu	3.34	1.92	1.28	2.42	0.98	0.90	2.23	2.09	1.07
Gd	10.3	6.42	4.85	9.06	2.91	3.16	8.20	6.57	3.25
Tb	1.64	1.10	0.89	1.52	0.52	0.55	1.55	1.25	0.60
Dy	9.88	6.80	5.78	9.52	3.32	3.27	9.81	7.74	3.85
Ho	2.02	1.42	1.30	1.76	0.73	0.68	2.10	1.68	0.83
Er	5.85	3.99	3.44	4.64	1.92	1.63	5.34	4.33	2.20
Tm	0.76	0.57	0.51	0.64	0.28	0.21	0.74	0.61	0.32
Yb	4.49	3.54	2.99	3.60	1.62	1.23	4.14	3.50	1.88
Lu	0.59	0.46	0.37	0.45	0.21	0.15	0.45	0.42	0.25
Nb	3.47	3.16	2.75	2.10	2.17	6.74	24.3	6.49	9.91
Hf	0.87	4.52	2.79	1.59	1.59	1.29	5.22	4.55	2.97
Ta	0.29	0.21	0.19	0.17	0.11	0.44	1.56	0.34	0.61
Th	9.28	5.72	3.21	5.09	0.16	1.00	2.13	0.75	0.80
U	0.51	0.66	0.34	0.15	0.06	0.11	0.51	0.21	0.17
Th/Ta	32.35	27.78	16.89	29.55	1.46	2.27	1.19	1.93	1.14
Th/Tb	5.66	5.19	3.58	3.35	0.32	1.81	1.19	0.52	1.16
Ba/Th	29.4	81.9	109.3	46.0	1005.8	104.2	41.5	202.7	78.2
Th/Nb	2.7	1.8	1.2	2.4	0.1	0.1	0.1	0.1	0.1
Zr/Nb	45.2	85.1	95.1	152.2	23.6	15.7	10.5	26.4	6.1
Nb/Yb	0.77	0.89	0.92	0.58	1.34	5.48	5.89	1.86	5.27
(La/Sm) _N	1.92	1.59	1.66	1.86	0.58	0.65	1.36	1.27	1.87
(La/Yb) _N	4.95	3.77	2.89	4.91	0.97	1.64	2.76	2.37	3.19

Fe₂O₃ = FeO x 0.15; Mg# = 100 x Mg/(Mg+Fe²⁺), where Mg = MgO/40.32 and Fe = FeO/71.85. Normalizing values for REE ratios are from Sun and McDonough (1989). Abbreviations: gsct- greenschist facies; bsct- blueschist facies; bas- metabasalt; and- metaand- desite; dac- metadacite; gra- metagranite; Fe-bas- metaferro-basalt; n.d.- not detected.

Kamariza Unit metavolcanic rocks

The Kamariza metavolcanic rocks (Table 1) range from basaltic to andesitic in composition with SiO_2 concentrations (normalized to secondary calcite-free basis) between 45.65 and 56.53 wt% and Mg# between 69 and 32. Compatible element concentrations are very low (Table 1, Fig. 5), whereas TiO_2 content is rather variable ($\text{TiO}_2 = 1.07$ - 2.18 wt%) and shows a slight decrease with decreasing Mg# (Fig. 5). Zr is also variable (22-228 ppm) and displays a weak positive correlation with decreasing Mg# (Fig. 5). Although metavolcanic rocks from the Kamariza Unit do not belong to a single cogenetic magmatic series, the elemental variation roughly shows a characteristic calc-alkaline trend of decreasing TiO_2 , MgO, Co, and V with increasing SiO_2 , Al_2O_3 , and P_2O_5 towards the more evolved rocks (Table 1, Fig. 5). The elemental variation described in the previous paragraph is consistent with fractionation of olivine, plagioclase, clinopyroxene, orthopyroxene, amphibole, and titanomagnetite.

The incompatible element abundance (Figs. 6a-c) ex-

hibits patterns which are very similar to those of oceanic calc-alkaline basalts (Pearce, 1983) with marked enrichment in Th, U, La, and Ce, and with depletion in Ta, Nb, Hf (and Ti). The magnitude of both positive and negative anomalies becomes stronger in the more evolved lavas (basaltic andesites and andesites). Samples SP15C and SP15D are strongly depleted in high field strength elements (HFSE) with respect to N-MORB (Fig. 6c). The chondrite-normalized REE abundances (Figs. 6d-f), of the Kamariza metavolcanic rocks have sub-parallel patterns, regularly decreasing from light REE (LREE) to heavy REE (HREE). The enrichment in LREE compared to HREE is rather uniform with $(\text{La}/\text{Yb})_N$ ratios ranging from 4 to 8. La generally varies from 50 to 150 times chondrite abundance, with the exception of samples SP15C and SP15D in which La is 22 and 29 times chondrite abundance. In addition, a slight negative Eu anomaly is observed in basaltic andesites and andesites. The REE patterns (Figs. 6d-f) are consistent with a calc-alkaline affinity for these rocks. Accordingly, in the discrimination diagrams shown in Fig. 7, most samples plot in the fields for calc-alkaline basalts.

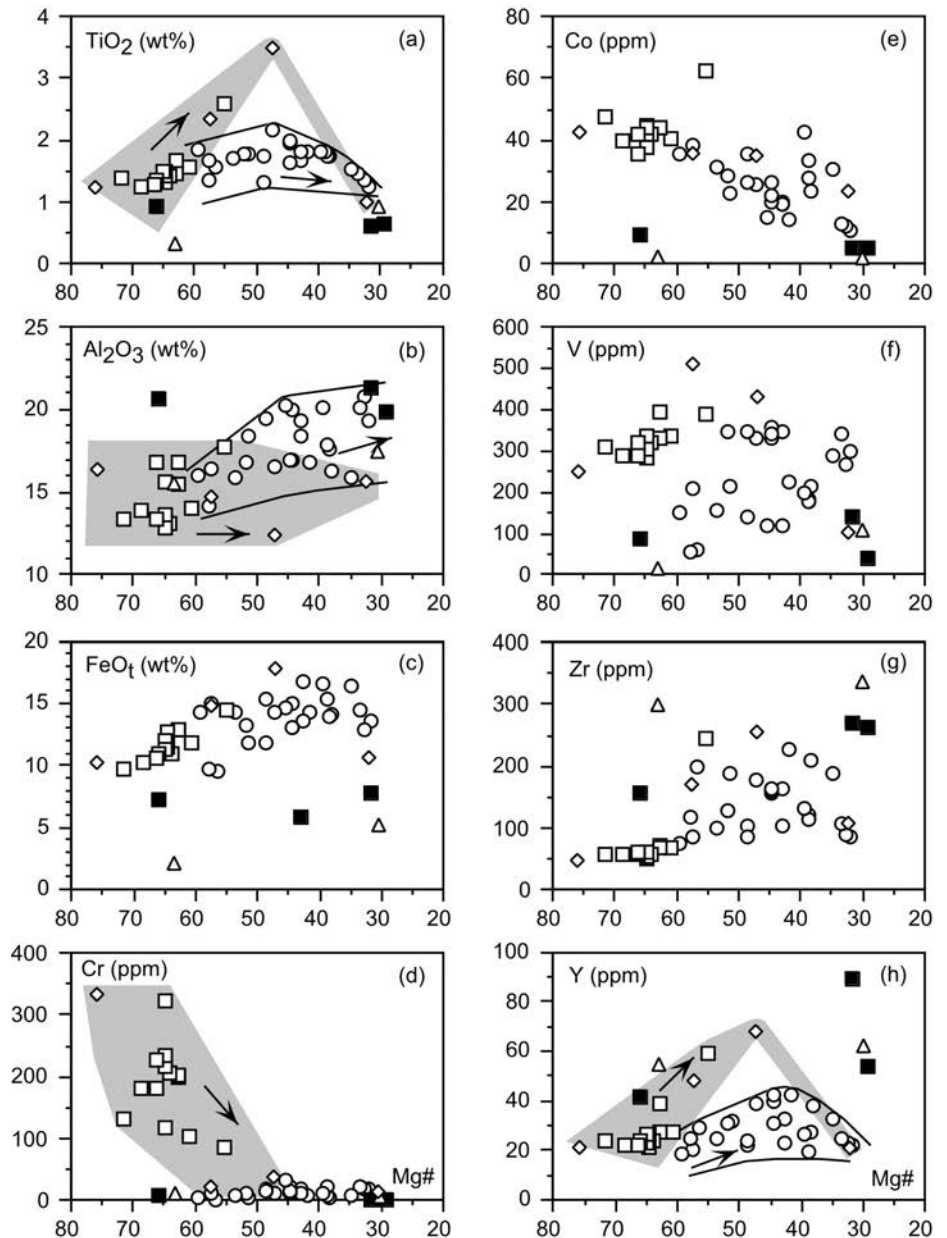


Fig. 5 - Variation of selected major and trace elements vs. Mg# for metavolcanic rocks from the Kamariza unit and metagranites from the Lavrion blueschist unit. Kamariza unit: metavolcanic rocks (open circles). Lavrion blueschist unit: calc-alkaline metavolcanic rocks (solid squares); calc-alkaline metagranites (open triangles); tholeiitic blueschist rocks (open diamonds); tholeiitic greenschist rocks (open squares). Major elements are recalculated on a secondary calcite-free basis. Rough fractionation trends for tholeiitic (grey field) and calc-alkaline (lines) metavolcanic rocks are also shown.

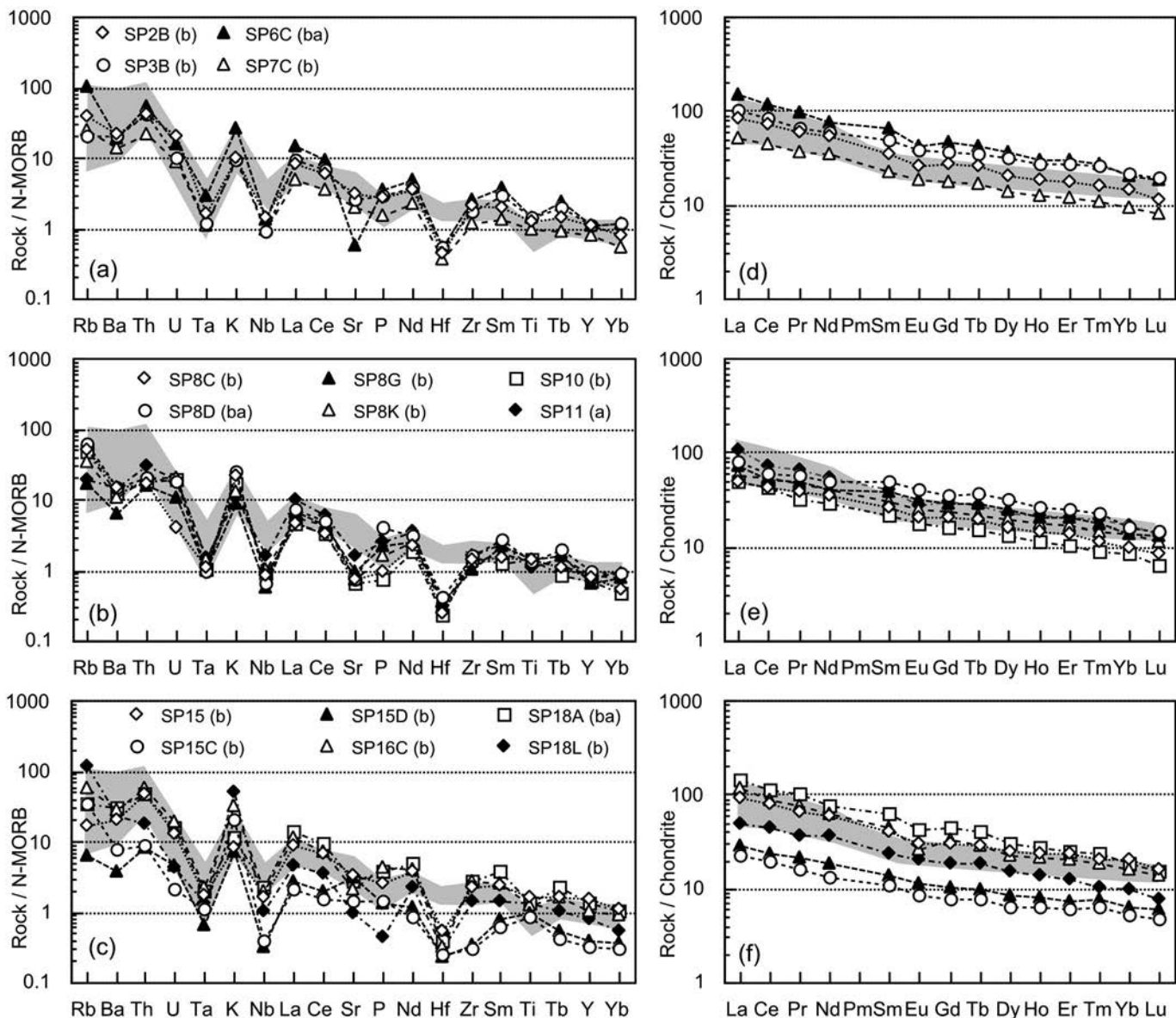


Fig. 6 - N-MORB normalized incompatible element (a, b, c) and chondrite-normalized REE patterns (d, e, f) for metamorphic rocks from the Kamariza Unit. All normalizing values are from Sun and McDonough (1989). Symbols for the REE patterns are the same as in the corresponding spiderdiagrams on the left. (b): metabasalt; (ba): metabasaltic andesite; (a): metaandesite. Gray fields represent the compositional variations of Triassic calc-alkaline basalts from various localities of the Hellenides (data from Capedri et al., 1997; Pe-Piper, 1998).

Lavrion blueschist Unit

Calc-alkaline metavolcanic rocks

These rocks (Table 2) range from basaltic to dacitic compositions with SiO_2 concentrations between 51.74 and 60.94 wt% and Mg# between 65.9 and 29.3. Compatible element concentrations and TiO_2 are very low (Table 2, Fig. 5). By contrast, Zr and Y are relatively high (Zr = 157-269 ppm; Y = 42-89 ppm) and display a relative increase with decreasing Mg# (Fig. 5). These rocks show incompatible element patterns characterized by depletion in Ta, Nb, Hf, and Ti and enrichment in Th, La, Ce, P, and Nd when compared to N-MORB compositions (Fig. 8a). These patterns are very similar to those of oceanic calc-alkaline basalts (Pearce, 1983).

The chondrite-normalized REE compositions display typical calc-alkaline patterns characterized by marked LREE enrichment with respect to HREE (Fig. 8b), with La_N/Yb_N ratios ranging from 3 to 5 and La/chondrite ratios

varying from 80 to 190. This conclusion is supported by the discrimination diagrams shown in Fig. 7, in which the metamorphic rocks plot in the fields for calc-alkaline basalts. The incompatible element and REE abundance is also quite similar to that observed in the Kamariza metamorphic rocks. Nonetheless, the magnitudes of both positive and negative anomalies observed in Fig. 8a, are more pronounced in the Lavrion blueschist Unit metamorphic rocks than in the Kamariza metamorphic rocks. In addition, the Lavrion blueschist Unit metamorphic rocks are characterized by strong negative Ti anomalies.

The calc-alkaline rocks from the Lavrion blueschist Unit have incompatible element composition very similar to those of the Triassic calc-alkaline volcanic rocks from the Hellenide belt (Capedri et al., 1997; Pe-Piper, 1998).

Calc-alkaline metagranitic rocks

The metagranites have SiO_2 concentrations of 64.04 and 71.95 wt%, with Mg# of 30.2 and 63.6. These rocks are

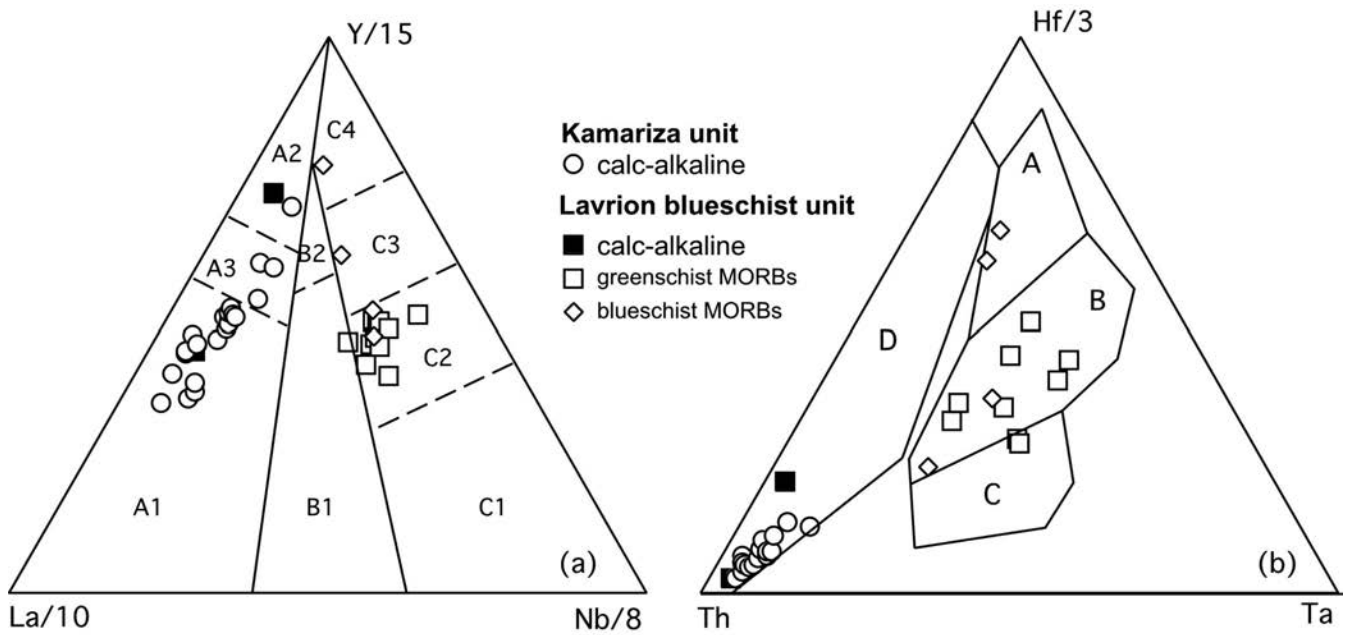


Fig. 7 - (a) La/10, Nb/8, Y/15 (Cabaniš and Lecolle (1989) and (b) Th, Ta, Hf/3 (Wood, 1980) discrimination diagrams for metavolcanic rocks from the Kamariza Unit and Lavrion blueschists Unit. Fields in (a). A1- calc-alkaline basalts; A2- volcanic arc tholeiites; A3- overlapping of A1 and A2; B1- continental basalts; B2- backarc basalts; C1- within-plate alkali basalts; C2 and C3- enriched mid-ocean ridge basalts (C2 more enriched than C3); C4- normal mid-ocean ridge basalts. Fields in (b). A- normal mid-ocean ridge basalts; B- transitional mid-ocean ridge basalts and within-plate tholeiites; C- within-plate alkali basalts; D- calc-alkaline basalts.

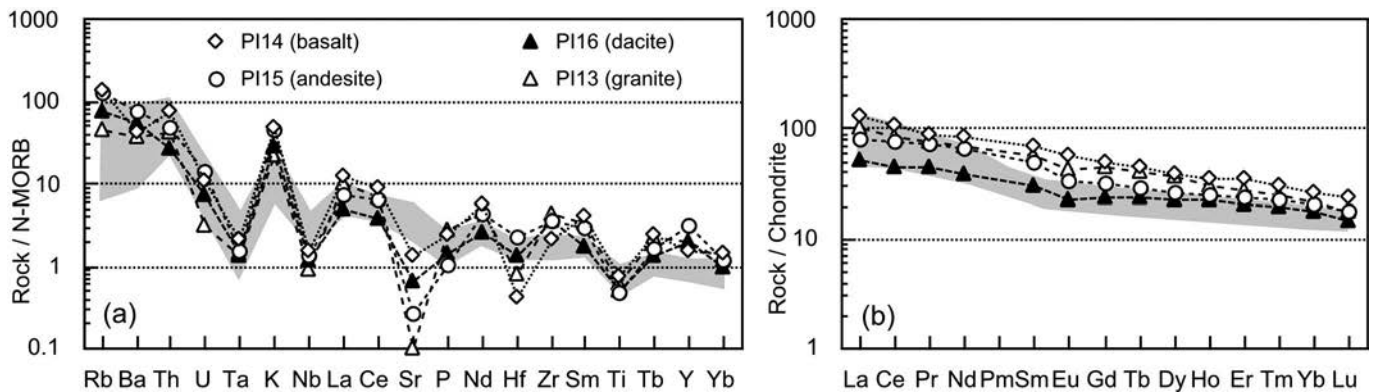


Fig. 8 - N-MORB normalized incompatible element (a) and chondrite-normalized REE patterns (b) for calc-alkaline rocks from the Lavrion blueschists Unit. All normalizing values are from (Sun and McDonough, 1989). Symbols for the REE patterns are the same as in the spiderdiagram. Gray fields represent the compositional variations of Triassic calc-alkaline basalts from various localities of the Hellenides (data from Capedri et al., 1997; Pe-Piper, 1998).

characterized by very low compatible element concentrations, high contents of Zr and Y, and variable amounts of TiO_2 , Al_2O_3 , FeO, and P_2O_5 (Table 2). Metagranites are characterized by depletion in Ta, Nb, Hf, and Ti and enrichment in Th, La, Ce, P, and Nd when compared to N-MORB composition (Fig. 8a). The chondrite-normalized REE compositions display patterns regularly decreasing from LREE to HREE and are characterized by marked LREE enrichment with respect to HREE (Fig. 8b), with $(\text{La}/\text{Yb})_N$ ratios ranging from 3 to 5. These geochemical features are comparable to those observed in granites generated in island arc settings (Pearce et al., 1984), and also similar to those of calc-alkaline metavolcanic rocks from the Lavrion blueschist Unit (Fig. 8).

Tholeiitic metabasaltic rocks

These rocks are mainly represented by chlorite-schists metamorphosed under greenschist facies conditions and

subordinately by blueschists. Since chlorite-schists derive from re-equilibration at lower pressure of blueschists, these two metamorphic rock types will be treated together in this section. Compositionally, they mainly include basalts and ferro-basalts, as well as subordinate andesites. SiO_2 concentrations range between 42.00 and 58.87 wt% and Mg# range between 76 and 32. They are characterized by variable, but generally high TiO_2 , P_2O_5 , and Y contents and relatively high incompatible element concentrations (Table 2, Fig. 5). These rocks display a tholeiitic character exemplified by the typical Ti and Fe increase from basaltic to ferro-basaltic compositions, followed by a decrease in the more evolved andesites (Figs. 5a, c). Although magmatic cogenetic relationships cannot be definitely established, the elemental variations and the whole geochemical characteristics are consistent with a magmatic evolution of the protoliths controlled by fractional crystallization of olivine, plagioclase, clinopyroxene, and Fe-Ti oxides.

N-MORB normalized spiderdiagrams (Fig. 9a-c) generally display regularly decreasing incompatible element patterns with no U nor Nb depletion, and are characterized by HFSE abundance ranging from 0.6 to 5 times typical N-MORB composition (Sun and McDonough, 1989). Most samples show REE patterns (Fig. 9d) slightly decreasing from LREE to HREE with LREE enrichment similar to E-MORB generated at a mid-ocean ridge from an enriched mantle source (Sun and McDonough, 1989), as testified by the $(La/Sm)_N$ and $(La/Yb)_N$ ratios (1.09-1.91 and 1.91-3.47, respectively).

By contrast, samples AF6 (metabasalt) and PL1 (metaandesite) show rather flat N-MORB normalized incompatible element patterns with lower abundance in low field strength elements (LFSE) relative to the other samples (Fig. 9a) and have depleted HFSE patterns at about 1 times N-MORB composition (Sun and McDonough, 1989). REE abundance

varies from 10 to 20 times that of chondrite, and displays LREE depletion with respect to medium REE (Fig. 9d), which is typical of N-MORB (Sun and McDonough, 1989). $(La/Sm)_N$ and $(La/Yb)_N$ ratios are 0.58 and 0.65 for metabasalt and metaandesite, respectively. These geochemical features suggest that the protoliths of samples AF6 and PL1 were generated in a mid-ocean ridge setting from a primitive MORB-type mantle source.

Although these two rocks display a common N-MORB signature, they are not genetically related because they are characterized by two distinct degrees of depletion of HREE with respect to medium REE (Fig. 9d), as well as other incompatible element ratios (Table 2). According to the discrimination diagrams of Fig. 7, tholeiitic metavolcanic rocks in both blueschist and greenschist facies fall in the E-MORB fields with the only exception of sample AF6, which displays a N-MORB composition.

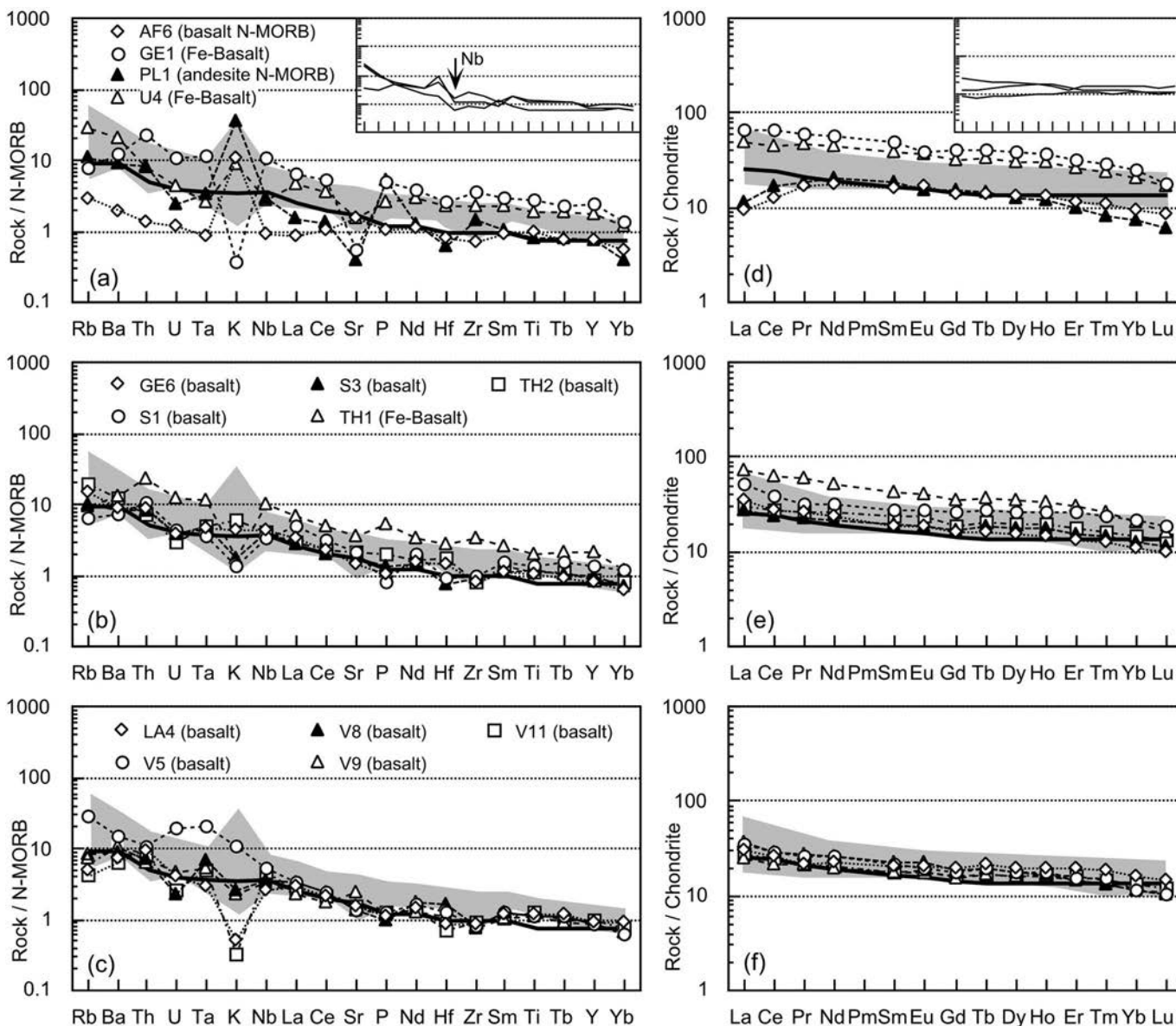


Fig. 9 - N-MORB normalized incompatible element (a, b, c) and chondrite-normalized REE patterns (d, e, f) for tholeiitic metavolcanic rocks from the Lavrion blueschists Unit. All normalizing values are from Sun and McDonough (1989). Symbols for the REE patterns are the same as in the corresponding spiderdiagrams on the left. (a, d): blueschist; (b, e and c, f): greenschist. Gray fields: compositional variations of Triassic E-MORBs from various sub-ophiolitic mélangé units from the Mirdita-Subpelagonian zone (Saccani and Photiades, 2005); heavy lines: compositions of the typical E-MORB (Sun and McDonough, 1989). Insets: compositional variations of similar rocks from the Ochi Unit, Evia Island (data from Katzir et al., 2000).

DISCUSSION

Occurrence and characteristics of HP/LT metamorphic rocks elsewhere in the Cyclades

HP/LT metamorphic rocks (including metaophiolites and metamorphosed ophiolitic mélanges) are widespread in the Cycladic area. However, most of the data published on these rocks deal with their metamorphic evolution, and few are the exhaustive studies on the magmatic evolution and geodynamic significance of the pre-metamorphic protoliths. Previous works on the pristine chemistry of Cycladic metamorphic rocks have been carried out in some of the Cycladic Islands, for example in Evia (Katzir et al., 2000), Siphnos (Mocek, 2001), Syros (Seck et al., 1996), Tinos (Brocker, 1991; Stolz et al., 1997), and Ikaria (Photiades, 2002; Pe-Piper and Photiades, 2006). The occurrence of calc-alkaline rocks associated with both E- and N-MORBs has been documented in the islands of Evia, Siphnos, Syros, and Tinos. In addition, a minor occurrence of boninitic rocks is also reported in Siphnos and Tinos. Most of the MORB-type metamorphic rocks bear SSZ geochemical characteristics (e.g., marked Nb depletion and LREE enrichment in Evia metabasalts, Katzir et al., 2000), which have allowed many authors to conclude that the protoliths have been generated in a backarc setting. Radiometric investigations for amphibolites from the Tinos metaophiolites (Patzak et al., 1994), report ages from 77 to 66 Ma, which may represent original or partially reset ages for the thrust on the ophiolitic metamorphic sole. By contrast, in Ikaria only metaophiolites with pure MORB geochemistry occur and have been interpreted as an Upper Cretaceous oceanic crust developed at a slow-spreading ridge (Photiades, 2002; Pe-Piper and Photiades, 2006).

Some authors (e.g., Mocek, 2001) suggested that the occurrence of both calc-alkaline and backarc basin basalts in the Cycladic HP/LT metamorphic rocks may reflect a geodynamic evolution of the Cycladic region, encompassing the formation of an island arc followed by opening of a backarc basin.

Nonetheless, geochronological data carried out on relict igneous zircons from the blueschist unit from the Cycladic islands of Folegandros and Sikinos (Photiades and Keay, 2003) indicate Triassic and Triassic-Jurassic ages of formation of the magmatic protoliths. These ages place a maximum age constrain on the sedimentation that generated the blueschists protoliths, that must have been deposited in the Triassic-Jurassic or possibly later. These data are consistent with fossil evidence of Triassic deposition for the schists from the blueschist units in the Cyclades (Dürr et al., 1978, and references therein). The presumed Eocene metamorphism age (Andriessen et al., 1979) places a minimum constraint on the time of sedimentation, while the recognition of Cretaceous metamorphic zircon overgrowths suggests that the rocks experienced a complicated pre-M1 history. For these reasons, it seems more likely that the sediments forming these rocks were deposited in the Triassic-Jurassic and underwent pre-M1 metamorphism that may be correlated to the Lower Cretaceous event, under epidote-amphibolite facies conditions that is recorded in the Pelagonian domain in continental Greece (Yarwood and Dixon 1977; Perraki et al., 2002). Photiades and Keay (2003) thus argued that these sediments were most likely deposited in an active tectonic environment similar to a modern-day backarc basin, accompanied by Triassic magmatism, before they underwent Cretaceous and then Tertiary metamorphism associated with the Alpine orogenesis.

Geochemical characteristics and geotectonic setting of the magmatic protoliths from the Lavrion area

The previous chapter has shown that protoliths of the metamorphic rocks studied in this paper represent two distinct geochemical groups: calc-alkaline rocks and MORB-type rocks. According to many authors (e.g., Pearce and Norry, 1979; Pearce, 1983), the compositional differences between these magma types are related to different source characteristics that can usually be associated to distinct tectono-magmatic settings of formation. Therefore, the characteristics and tectonic setting of the possible mantle sources will be evaluated for both rock types in order to assess their relationship and an eventual common geologic evolution.

The incompatible element distribution of calc-alkaline rocks (Figs. 6 and 8) indicates that they originated from a depleted mantle source(s) further enriched by a subduction component. In particular, calc-alkaline metavolcanic rocks from both the Kamariza and Lavrion Units display a Th enrichment (Fig. 10) typical of subduction components. In addition, calc-alkaline rocks from the Kamariza Unit are characterized by Th/Nb ratios greater than 1, which are the typical values for enrichment due to the sediment component (Woodhead et al., 1998). The calc-alkaline metavolcanic rocks studied in this paper are similar to Triassic calc-alkaline volcanic rocks (Figs. 6, 8, 10) from several localities of the Hellenides (Capedri et al., 1997; Pe-Piper, 1998, and references therein), which are interpreted as having originated in an extensional setting from a mantle source with subduction-related geochemical characteristics, inherited from a Hercynian subduction below Gondwana (Pe-Piper, 1998). This conclusion is consistent with the generally high Zr/Y

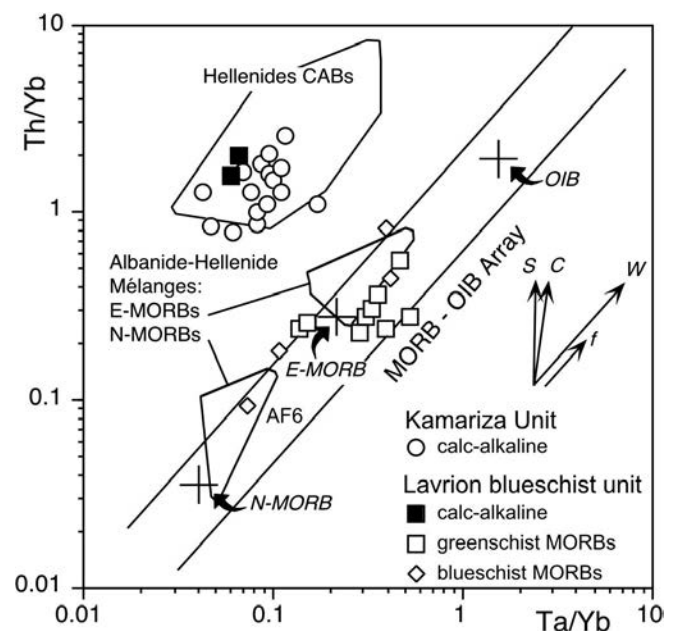


Fig. 10 - Th/Yb vs. Ta/Yb diagram for metavolcanic rocks from the Kamariza Unit and Lavrion blueschists Unit. Modified after Pearce (1983). Crosses represent the compositions of modern normal mid-ocean ridge basalt (N-MORB), enriched mid-ocean ridge basalt (E-MORB) and within-plate ocean island basalt (OIB) (data from Sun and McDonough, 1989). Compositional fields of Triassic calc-alkaline basalts (CABs) from various localities of the Hellenides (Pe-Piper, 1998; Pe-Piper and Piper, 2002), as well as Triassic E- and N-MORBs from sub-ophiolitic mélanges units from the Albanide-Hellenide belt (Saccani and Photiades, 2005) are reported for comparison. The vectors of enrichment are: S- subduction zone; C- crustal contamination; W- within-plate; f- fractional crystallization.

ratios (>3) observed in the calc-alkaline metavolcanic rocks, which are considered by Pearce (1983) a measure of within-plate enrichment.

The chemistry of the MORB-type basalts suggests melt generation by partial melting of both a MORB-type mantle source variably enriched in low field strength elements and LREE (E-MORBs), and of a primitive asthenospheric source (N-MORBs).

E-MORB metavolcanic rocks from the Lavrion Unit plot in Fig. 10 in the N-MORB-OIB array, roughly close to the typical E-MORB composition (Sun and McDonough, 1989), suggesting that they have been partially generated by melting of a MORB source chemically modified by a plume component. The Th/Yb and Ta/Yb ratios included in the MORB-OIB array also suggest that these rocks were generated without any detectable influence of continental crust contamination. The marked enrichment in large ion lithophile elements (LILE) and LREE observed in Fig. 9 is in accordance with this conclusion.

The metavolcanic rocks with E-MORB geochemistry are similar to the Triassic E-MORBs included in the sub-ophiolitic mélangé units of the Mirdita-Subpelagonian zone (Figs. 9, 10), which have been interpreted by Saccani and Photiades (2005) as originated from the interaction between uprising depleted oceanic asthenosphere and OIB-type plume material during the initial stage of spreading of the Pindos oceanic basin. Although the data presented in this paper do not allow to define the original tectono-magmatic setting, a similar conclusion can be reasonably postulated for the E-MORBs from the Lavrion blueschist Unit.

Metabasalt AF6, showing N-MORB chemistry, plots towards the typical N-MORB composition in Fig. 10. The Th/Yb and Ta/Yb ratios (Fig. 10) and LREE depletion (Fig. 9d) for N-MORB rocks are very similar to those of N-MORBs from various ophiolitic mélangés of the Hellenides (Saccani and Photiades, 2005), and are generally compatible with a genesis from primary magmas originating from depleted N-MORB type sub-oceanic mantle sources, with little influence of enriched OIB-type material.

The calc-alkaline-MORBs association from various blueschists units elsewhere in the Cyclades has been interpreted as reflecting the formation of an island arc and the opening of a backarc basin in the Cycladic region during the Jurassic-Cretaceous (e.g., Mocek, 2001). The SSZ geochemical signatures, typical of backarc basin basalts observed in MORB protoliths from the Cyclades (Brocker, 1991; Stolz et al., 1997; Mocek, 2001), strongly support this conclusion. Analogously, marked Nb negative anomalies and, in some cases, HFSE depletion observed in MORB protoliths of the blueschists from the Evia Island (inset in Fig. 9) are interpreted as SSZ features, which testify for a backarc setting of formation (Katzir et al., 2000).

However, according to Photiades and Carras (2001), the Kamariza Unit has pre-metamorphic geological features typical of the Pelagonian domain. For example, its lithological sequence is not a continuous calcareous sedimentary succession from Triassic to Eocene (as in the case of the External Hellenides) but it presents an evident hiatus during the Late Jurassic. This implies that the Kamariza Unit, like the Pelagonian domain, was affected by an orogenic episode during the Late Jurassic. In addition, these authors also suggested that the protoliths of both the Kamariza and Lavrion blueschist Units were incorporated into sedimentary sequences during two different tectonic events, prior to the Eocene HP/LT metamorphic event.

Accordingly, the magmatic protoliths of the HP/LT metamorphic rocks from the Lavrion area most likely recorded some of the Triassic magmatism of the Pelagonian domain, which includes: (1) calc-alkaline rocks associated with continental rifting between the Apulian and Pelagonian microplates (Pe-Piper, 1998); (2) alkali basalts, commonly referred either to oceanic island or continental rift settings (Pe-Piper and Piper, 2002, and references therein; Saccani and Photiades, 2005); (3) both E- and N-MORB associated with the initial stage of the Pindos oceanic spreading (Saccani and Photiades, 2005).

In fact, calc-alkaline metavolcanic rocks from the Lavrion area display close similarities with Triassic calc-alkaline rocks from the Pelagonian domain. Accordingly, the geochemical features of MORB protoliths from the Lavrion blueschist Unit can be compared to Triassic MORB-type volcanic rocks from the Pindos oceanic basin. They reflect a genesis in a mid-ocean ridge setting where depleted asthenospheric sources and enriched OIB sources variably interacted. By contrast, the SSZ geochemical features typical of MORB protoliths from blueschists from the Cyclades and Evia islands were not found in the MORB protoliths from the Lavrion area. The above evidence suggests that calc-alkaline and MORB metamorphic rocks from the Lavrion area cannot be correlated to analogous rocks from other localities of the Cycladic zone.

In summary, the magmatic rocks included into the Lavrion HP/LT metamorphic rocks were emplaced during the Triassic along the border between the Pelagonian continental margin and the newly formed Pindos oceanic basin. During the Middle-Upper Jurassic closure of the Pindos ocean, these magmatic rocks were probably incorporated into mélangés together with and/or within Pelagonian-type successions, which were finally involved in the Eocene HP/LT metamorphic events that affected the Cycladic zone.

CONCLUSIONS

The Lavrion area largely consists of HP/LT metamorphic rocks, which are found in two superposed tectonic units (Kamariza Unit and Lavrion blueschist Unit) overlain by non-metamorphic sequences belonging to the Pelagonian Zone. These units underwent the Eocene HP/LT metamorphic event and the Upper Oligocene-Lower Miocene medium-pressure metamorphic overprint, which are typical for the Cycladic zone of the Hellenides. From the study of the magmatic protoliths of the Kamariza and Lavrion blueschist Units the following conclusions can be drawn:

(1) The Kamariza Unit includes schists with metavolcanic blocks showing calc-alkaline affinity, whereas in the Lavrion blueschist Unit only subordinate metagranites and metavolcanic rocks have calc-alkaline affinity, while the metavolcanic rocks with MORB composition, mainly E-MORB and rare N-MORB are widespread

Calc-alkaline rocks from both Kamariza and Lavrion blueschist Units display marked enrichment in Th, U, and LREE and depletion in Ta, Nb, Hf and Ti, which testify a genesis from a depleted mantle source further enriched by subduction components. E-MORBs are characterized by Th, U, Ta, Nb and marked LREE enrichments, which imply a genesis from a depleted asthenospheric source modified by an OIB component. N-MORBs display incompatible element abundances and LREE depletion with respect to HREE, which are typical for rocks generated in a mid-ocean

ridge setting from a primitive asthenospheric source. Contrary to what is observed in MORB-type rocks from various blueschist units from the Cycladic zone, no SSZ geochemical signature can be observed in the equivalent protoliths from the Lavrion area.

(2) Geological evidence (Photiades and Carras, 2001; Photiades et al., 2004) suggests that the Lavrion metamorphic Units represent Triassic Pelagonian sequences metamorphosed under the HP/LT conditions typical of the Cycladic zone. The geochemical and petrological similarities between the Lavrion calc-alkaline protoliths and the Triassic calc-alkaline rocks associated with the Gondwana rift (Pe-Piper, 1998), as well as those between the Lavrion MORB-type protoliths and the MORBs forming the Subpelagonian ophiolitic mélanges, further support this conclusion.

(3) The magmatic protoliths of the Lavrion HP/LT metamorphic rocks are compatible with a geodynamic evolution encompassing a Triassic continental rift followed by an early oceanization stage along the Pelagonian margin, during which these rocks were emplaced on the border between the Pelagonian continental margin and the Pindos oceanic basin. These rocks were probably incorporated into mélanges during the Jurassic closure of the Pindos basin, and finally involved in the Eocene and Upper Oligocene-Lower Miocene metamorphic events that affected the Cycladic zone.

(4) The protoliths of the HP/LT metamorphic rocks from the Cyclades represent the magmatic events that accompanied the Cretaceous closure of the Pindos oceanic basin (e.g., Mocek, 2001). By contrast, similar rocks in the Lavrion area most likely record the magmatic events that occurred during the early stages of opening of this oceanic basin.

ACKNOWLEDGEMENTS

This research was financially supported by MURST-COFIN 2000 and by IGME (Athens). Chemical analyses have been performed by R. Tassinari. Many thanks go to G. Pe-Piper and E. Piluso for their constructive reviews.

REFERENCES

- Alexopoulos A., Lekkas S. and Moraïti E., 1998. On the occurrence of a non-metamorphic Upper Eocene-Lower Oligocene clastic sequence, wedged between the allochthon and the relative autochthon system of Attiki (Greece). *Bull. Geol. Soc. Greece*, 32 (1): 79-84.
- Altherr R., Schliestedt M., Okrusch M., Seidel E., Kruezer H., Harre W., Lenz H., Wendt J. and Wagner G.A., 1979. Geochronology of high-pressure rocks on Sifnos (Cyclades, Greece). *Contrib. Mineral. Petrol.*, 70: 245-255.
- Altherr R., Kruezer H., Wendt J., Lenz H., Wagner G.A., Keller J., Harre W. and Hohndorf A., 1982. A Late Oligocene/Early Miocene high temperature belt in the Attic-Cycladic Crystalline Complex (SE Pelagonian, Greece). *Geol. Jahrb.*, E23: 97-164.
- Andriessen P.A.M., Boelrijk N.A.I.M., Hebeda E.H., Priem H.N.A., Verdurmen E.A.T. and Verschure R.H., 1979. Dating the events of metamorphism and granitic magmatism in the Alpine orogeny of Naxos (Cyclades, Greece). *Contrib. Mineral. Petrol.*, 69: 215-225.
- Arikas K., Pape M., Serelis K. and Tsagalidis A., 2001. Petrological-mineralogical study of metabasic rocks (prasinities) of the Lavreotiki area and their geotectonic environment. *Bull. Geol. Soc. Greece*, 34 (3): 901-910 (in Greek with English abstract).
- Baltatzis E., 1981. Contact metamorphism of a calc-silicate hornfels from Plaka area, Laurium, Greece. *N. Jb. Miner., Mh. H.*, 11: 481-488.
- Baltatzis E., 1996. Blueschist-to-greenschist transition and the P-T path of prasinities from the Lavrion area, Greece. *Mineral. Mag.*, 60: 551-561.
- Bortolotti V., Carras, N., Chiari M., Fazzuoli M., Marcucci M., Photiades A. and Principi G., 2003. The Argolis Peninsula in the palaeogeographic and geodynamic frame of the Hellenides. *Ophioliti*, 28: 79-94.
- Brocker M., 1991. Geochemistry of metabasic HP/LT rocks and their greenschist facies and contact metamorphic equivalents, Tinos Island (Cyclades, Greece). *Chem. Erde*, 51: 155-171.
- Cabanis B. and Lecolle M., 1989. Le diagramme La/10-Y/15-Nb/8: un outil pour la discrimination des séries volcaniques et la mise en évidence des processus de mélange et/ou contamination crustale. *C. R. Acad. Sci. Paris Sci. Terre Plan.*, 309: 2023-2029.
- Capedri S., Toscani L., Grandi R., Venturelli G., Papanikolaou D. and Skarpelis N., 1997. Triassic volcanic rocks of some type-localities from the Hellenides. *Chem. Erde*, 57: 257-276.
- Dermitzakis M., and Papanikolaou D., 1980. Paleogeography and geodynamics of the Aegean region during the Neogene. VII Int. Cong. on Med. Neog., Athens 1979, *Ann. Géol. Pays Hellén.*, Tome hors série, fasc. 4: 245-289.
- Durr S.T., Altherr R., Keller J., Okrusch M. and Seidel E., 1978. The median Aegean crystalline belt: Stratigraphy, structure, metamorphism, magmatism. In: Closs et al. (Eds.), *Alps, Apennines, Hellenides, Mediterranean Orogens*, 38: 455-477.
- Ferrière J., 1982. Paleogéographies et tectoniques superposées dans les Hellenides Internes: Les massifs de l'Othrys et du Pélion (Grèce continentale). *Soc. Géol. Nord.*, Publ. 8, Ville-neuve-d'Ascq.
- Jackson M.L., 1958. Soil chemical analysis, Prentice-Hall, 498 pp.
- Katsikatos G., 1977. La structure tectonique d'Attique et de l'île d'Eubée. VI Coll. Geology of the Aegean region, Athens, 1: 211-220.
- Katsikatos G., Migiros G., Triantaphyllis M. and Mettos A., 1986. Geological structure of internal Hellenides. *Geol. Geoph. Res., Spec. Issue*, p. 191-212, I.G.M.E., Athens.
- Katzir Y., Avigad D., Matthews A., Garfunkel Z. and Evans B.W., 2000. Origin, HP/LT metamorphism and cooling of ophiolitic mélanges in southern Evia (NW Cyclades), Greece. *J. Metam. Geol.*, 18: 699-718.
- Lachance G.R. and Trail R.J., 1966. Practical solution to the matrix problem in X-ray analysis. *Can. Spectrosc.*, 11: 43-48.
- Leleu M., 1966. Données nouvelles sur la paléogéographie et les rapports des séries métallifères du Laurium (Attique, Grèce). *C. R. Acad. Sci. Paris*, 262: 2008-2011.
- Leleu M., 1969. Essai d'interprétation thermodynamique en métalogénie: les minéralisations karstiques du Laurium (Grèce). *Bull. B.R.G.M.*, 2^e s., 4: 1-66.
- Leleu M. and Neumann M., 1969. L'âge des formations d'Attique (Grèce): du Paléozoïque au Mésozoïque. *C. R. Acad. Sci. Paris*, 268: 1361-1363.
- Maluski H., Vergely P., Bavay D., Bavay Ph. and Katsikatos G., 1980. ⁴⁰Ar/ ³⁹Ar dating of glaucophanes and phengites in Southern Euboea (Greece) geodynamic implications. *Bull. Soc. Géol. France*, 23 (5): 469-476.
- Marakis G., 1968. Remarks on the age of sulfide mineralisation in Cyclades area. *Ann. Géol. Pays Hellén.*, 19: 695-700.
- Marinos G., 1955. Das alter der kristallinen Schichten Attikas. *Bull. Geol. Soc. Greece*, 2 (1): 1-13.
- Marinos G. and Petrascheck W.E., 1956. Laurium. *Geol. Geophys. Res.*, 4: 1-247. I.G.S.R., Athens.
- Marinos G., Katsikatos G., Mercier J., Vergely P., Aubouin J., Symeonidis N. and Marcopoulou-Diacantoni A., 1977. Réunion extraordinaire de la Soc. Géol. Grèce en Eubée et en Attique (21-24 septembre 1976). *Bull. Soc. Géol. France*, 19 1: 103-116.
- Mocek B. 2001. Geochemical evidence for arc-type volcanism in the Aegean Sea: the blueschist unit of Siphnos, Cyclades (Greece). *Lithos*, 57: 263-289.

- Papanikolaou D., 1984. The three metamorphic belts of the Hellenides: a review and a kinematic interpretation. In: J.E. Dixon and A.H.F. Robertson (Eds.), *The geological evolution of the Eastern Mediterranean*, Geol. Soc. London Spec. Publ., 17: 551-561.
- Paraskevopoulos G., 1957. Die gesteine des horizontes des Kaissariani-schiefers im Pentelikongebirge. *Ann. Géol. Pays Hellén.*, 8: 233-245
- Patzak M., Okrusch M., and Kreuzer H., 1994. The Akrotiri Unit on the Island of Tinos, Cyclades, Greece: witness to a lost terrane of Late Cretaceous age. *N. Jahr. Geol. Pal., Abh.*, 194: 211-52.
- Pearce J.A., 1983. Role of the Sub-continental lithosphere in magma genesis at active continental margin. In: C.J. Hawkesworth and M.J. Norry (Eds.), *Continental basalts and mantle xenoliths*. Shiva, Nantwich, p. 230-249.
- Pearce J.A. and Norry M.J., 1979. Petrogenetic implications of Ti, Zr, Y, and Nb variations in volcanic rocks. *Contrib. Mineral. Petrol.*, 69: 33-47.
- Pearce J.A., Harris N.B.W. and Tindle A.G., 1984. Trace element discrimination diagrams for the tectonic interpretation of granitic rocks. *J. Petrol.*, 25: 956-983.
- Pe-Piper G., 1998. The nature of Triassic extension-related magmatism in Greece: Evidence from Nd and Pb isotope geochemistry. *Geol. Mag.*, 135: 331-348.
- Pe-Piper G. and Piper D.J.W., 2002. *The igneous rocks of Greece. The anatomy of an orogen*. Gebrüder Borntraeger, Berlin, 573 pp.
- Pe-Piper G. and Photiades A. 2006. Geochemical characteristics of the Cretaceous ophiolitic rocks of Ikaria island, Greece. *Geol. Mag.*, in press.
- Perraki M., Mposkos E., Hoinkes G. and Orfanoudaki A., 2002. Amphibole zonation in glaucophane-schists, epidote-amphibolites and albite-gneisses as a guide to the metamorphic evolution of the Pelagonian zone, NE Thessaly, Greece. *Geol. Carpathica*, 53: 164-165.
- Photiades A., 2002. The ophiolitic molasse unit of Ikaria Island (Greece). *Turkish J. Earth Sci.*, 11: 27-38.
- Photiades A., 2003. Geological structure of the Lavreotiki area (Attica, Greece). In: A. Demetriades (Ed.), *Lavreotiki Excursion Guide*, 29th August 2003, Excursion leaders A. Demetriades, A. Photiades and C. Panagopoulos, 7th Biennial S.G.A. Meeting "Mineral Exploration and Sustainable Development, August 24-28, 2003, Athens, Greece.
- Photiades A., 2004. Geological mapping revision of the Vermion Mountain (Internal Hellenides, Greece). *Proceed. 5th Intern. Symp. on Eastern Mediterranean Geol.*, Thessaloniki, Greece, 14-20 April 2004, 1: 161-164.
- Photiades A. and Carras N., 2001. Stratigraphy and geological structure of the Lavrion area (Attica, Greece). *Bull. Geol. Soc. Greece*, 34 (1): 103-109.
- Photiades A. and Pomoni-Papaioannoy F., 2001. Contribution to the structural study of the Rhodian ophiolites, Vourinos Massif. *Bull. Geol. Soc. Greece*, 34 (1): 111-118.
- Photiades A. and Keay S. 2003. Geochronological data for Sikinos and Folegandros metamorphic units (Cyclades, Greece): their tectono-stratigraphic significance. *Bull. Geol. Soc. Greece*, 35: 35-45.
- Photiades A., Carras N. and Mavridou F., 2004. Geological map of Greece in scale 1:50.000 "Lavrion-Makronisos" sheet. *Ins. Geol. Mineral. Explor.* Athens, Greece.
- Ring U., LAYER P.W. and Reischmann T. 2001. Miocene high-pressure metamorphism in the Cyclades and Crete, Aegean Sea, Greece: Evidence for large-magnitude displacement on the Cretan detachment. *Geology*, 29: 395-398.
- Saccani E., Padoa E. and Photiades A., 2003. Triassic mid-ocean ridge basalts from the Argolis Peninsula (Greece): new constraints for the early oceanization phases of the Neo-Tethyan Pindos basin. In: Y. Dilek and P.T. Robinson (Eds.), *Ophiolites in earth history*. Geol. Soc. London Spec. Publ., 218: 109-127.
- Saccani E. and Photiades A. 2005. Petrogenesis and tectono-magmatic significance of volcanic and subvolcanic rocks in the Albanide-Hellenide ophiolitic mélanges. In: Y. Dilek, Y. Ogawa, V. Bortolotti and P. Spadea (Eds.) *Evolution of Ophiolites in convergent and divergent plate boundaries*. Island Arc, 14: 494-516.
- Seck H.A., Kotz J., Okrusch M., Seidel E. and Stosch H.G. 1996. Geochemistry of a meta-ophiolite suite: an association of metagabbros, eclogites and glaucophanotes on the island of Syros, Greece. *Eur. J. Mineral.*, 8: 607-623.
- Sindowski K.H., 1948. *Der geologische Bau von Attika*. *Ann. Géol. Pays Hellén.*, 2: 163-218.
- Stolz J., Engi M. and Rickli M., 1997. Tectonometamorphic evolution of SE Tinos, Cyclades, Greece. *Schw. Miner. Petrogr. Mitt.*, 77: 209-31.
- Sun S.-S. and McDonough W.F., 1989. Chemical and isotopic systematics of oceanic basalts: implications for mantle composition and processes. In: A.D. Saunders and M.J. Norry (Eds.), *Magmatism in the ocean basins*, Geol. Soc., London, Spec. Publ., 42: 313-345.
- Vergely P., 1984. *Tectonique des ophiolites dans les Hellénides Internes (déformations, métamorphismes et phénomènes sédimentaires). Conséquences sur l'évolution des régions téthysiennes occidentales*. Thèse État Sci. Nat., Univ. Paris-Sud, 649 pp.
- Wood D.A., 1980. The application of a Th-Hf-Ta diagram to problems of tectonomagmatic classification and to establishing the nature of crustal contamination of basaltic lavas of the British Tertiary volcanic province. *Earth Planet. Sci. Lett.*, 50: 11-30.
- Woodhead J.D., Eggins S.M. and Johnson R.W. 1998. Magma genesis in the New Britain Island arc: further insights into melting and mass transfer processes. *J. Petrol.*, 39: 1641-1668.
- Yarwood G.A. and Dixon J.E., 1977. Lower Cretaceous and younger thrusting in the Pelagonian rocks of the High Pieria, Greece. 6th Colloquium on the Geology of the Aegean region, 1: 269-280.